Accepted Manuscript

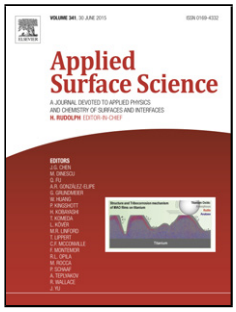

Title: Adsorption of bentazon on CAT and CARBOPAL activated carbon: Experimental and computational study

Authors: Agustín Spaltro, Sandra Simonetti, Silvia Alvarez Torrellas, Juan Garcia Rodriguez, Danila Ruiz, Alfredo Juan, Patricia Allegretti

PII: S0169-4332(17)32934-3
DOI: https://doi.org/10.1016/j.apsusc.2017.10.011
Reference: APSUSC 37354

To appear in: *APSUSC*

Received date: 23-5-2017
Revised date: 17-8-2017
Accepted date: 2-10-2017

Please cite this article as: Agustín Spaltro, Sandra Simonetti, Silvia Alvarez Torrellas, Juan Garcia Rodriguez, Danila Ruiz, Alfredo Juan, Patricia Allegretti, Adsorption of bentazon on CAT and CARBOPAL activated carbon: Experimental and computational study, Applied Surface Science https://doi.org/10.1016/j.apsusc.2017.10.011

Adsorption of bentazon on CAT and CARBOPAL activated carbon: experimental and computational study

[1,2]Agustín Spaltro; [3,4] Sandra Simonetti; [5]Silvia Alvarez Torrellas; [5]Juan Garcia Rodriguez; [1,2]Danila Ruiz; [3]Alfredo Juan; [1]Patricia Allegretti

[1]CEDECOR (Centro de Estudio de Compuestos Orgánicos) Facultad de Ciencias Exactas, Universidad Nacional de La Plata (UNLP), Calle 115 y 47, (1900) La Plata, Argentina.

[2]CONICET (Consejo Nacional de Investigaciones Científicas y Técnicas), Argentina

[3]Instituto de Física del Sur (IFISUR), Departamento de Física, Universidad Nacional del Sur (UNS), CONICET, Av. L. N. Alem 1253,B8000CPB - Bahía Blanca, Argentina.

[4]Universidad Tecnológica Nacional (UTN), 11 de Abril 461, B8000LMI - Bahía Blanca, Argentina.

[5]Grupo de Catálisis y Procesos de Separación (CyPS), Departamento de Ingeniería Química, Facultad de Ciencias Químicas, Universidad Complutense de Madrid, Avda. Complutense s/n, 28040 Madrid, Spain

Graphical Abstract

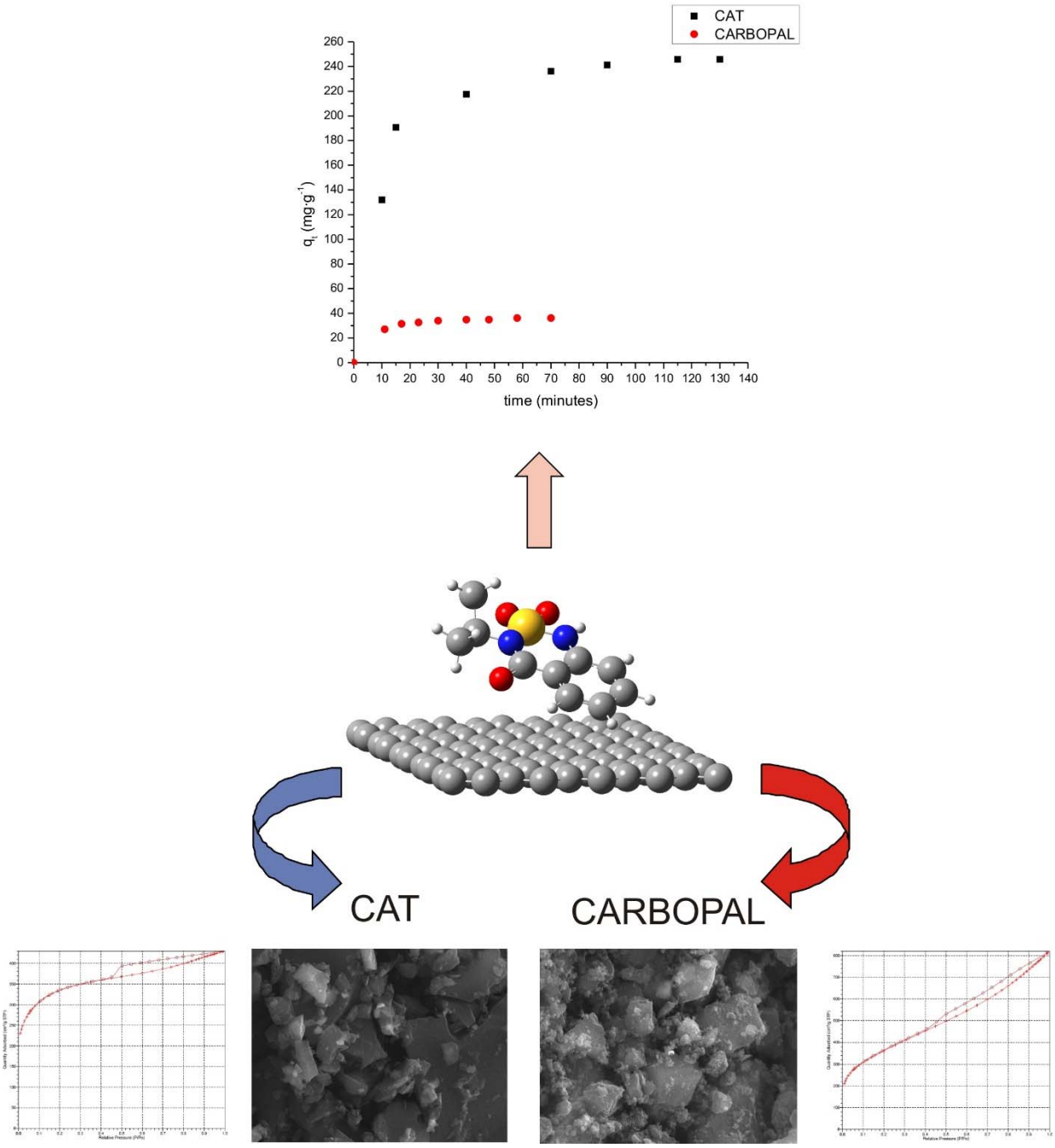

Highlights

- Kinetics indicates pesticide followed pseudo-second-order model on both adsorbent.
- Adsorption capacity decreases with the increase of temperature, pH and ionic strength.
- Adsorption capacity at 293 K is 391.65 mg·g^{-1} on CAT and 185.07 mg·g^{-1} on CARBOPAL.
- Data adapt Langmuir on CAT and Guggenheim–Anderson–de Boer isotherm on CARBOPAL.
- Flat bentazon is major stabilized and trapped through π-π dispersive interactions.

Abstract

Removal of the bentazon by adsorption on two different types of activated carbon was investigated under various experimental conditions.Kinetics of adsorption is followed and the adsorption isotherms of the pesticide are determined. The effects of the changes in pH, ionic strength and temperature are analyzed. Computational simulation was employed to analyze the geometry and the energy of pesticide absorption on activated carbon. Concentration of bentazon decreases while increase all the variables, from the same initial concentration. Experimental data for equilibrium was analyzed by three models: Langmuir, Freundlich and Guggenheim–Anderson–de Boer isotherms. Pseudo-first and pseudo-second-order kinetics are tested with the experimental data, and pseudo-second-order kinetics was the best for the adsorption of bentazon by CAT and CARBOPAL with coefficients of correlation R^2 = 0.9996 and R^2 = 0.9993, respectively. The results indicated that both CAT and CARBOPAL are very effective for the adsorption of bentazon from aqueous solutions, but CAT carbon has the greater capacity.

Keywords

bentazon, carbonaceous adsorbents, adsorption, isotherm model, computational simulation

1. Introduction

The rapid technological progresses have resulted in a huge amount of wastewater from industrial processes that need to be removed before discharge into the environment. Inorganic and organic pollutants dissolved in aqueous solutions are hazardous because of their toxicity, even at low concentrations. The global increase of polluted waters seriously threatens human health and the environment. Regulatory agencies have determined maximum allowable concentration of the contaminants in drinking water to overcome the problem. Clean water is one of the most important issues worldwide because of continuing economic development and the steady increase in the global population. However, clean water resources are decreasing every day, because of contamination with pollutants including organic chemicals. Since the mid-twentieth century, there has been growing concern about the care of the environment, which has led to the establishment of rigid limits on specific contaminants that affect health. Likewise, the increase in the number of habitants of the planet has caused an imperative need to produce more quantity and quality of food resources for future generations. For decades, tons of biologically active substances, synthesized for use in agriculture, industry, medicine, etc., have been dumped into the environment inadequately. Together with the problem of water pollution, there is a shortage of this non-renewable resource due to climate change and the increasing desertification that the planet is suffering.

Bentazon (3-isopropyl -(1H)-2,1,3-benzothiadiazin -4(3H)-one-2,2-dioxide, Fig.1) is the active compound in BASAGRAN®, registered trademark by BASF, in aqueous solution at 48 and 60%. It is one of the most commonly used herbicides in agriculture and gardening. Bentazon is a broad-spectrum post-emergence herbicide belonging to the chemical group of benzothiadiazinones used for the selective control of broadleaf weeds, in alfalfa, rice, pea, onion, asparagus, flax, maize, peanut, potatoes, beans, soybeans, sorghum, fruit trees and other crops. Being a contact herbicide, it affects the parts of the plant where it is applied. It acts by contact on the herbs of the broad leaf (dicotyledons) and some non-rhizomatous cyperaceae, absorbed by the foliage and very weakly translocated from it. To a lesser extent, the roots absorb it, in this case, it translates acroptically into the xylem. In all cases it is rapidly metabolized, conjugated and incorporated as natural components of the plant. It prevents the photos in Hill's reaction. The selectivity appears by the detoxifying action produced by a conjugation with glucose, the characteristic action of herbicide tolerant plants. The results are appreciated within the week following the application. It is absorbed by leaves and has a short herbicidal effect, inhibiting the transfer of electrons during photosynthesis causing oxidative stress by accumulation of the photosynthetic electrons in the PSII system [1]. Its selectivity is based on the ability of crop plants to rapidly metabolize bentazon to 6-OH- and 8-OH- bentazon interacting these with the synthesized sugars [2]. Bentazon is stable to hydrolysis and is very mobile in soil therefore it has the potential to contaminate surface water. On floor, under aerobic conditions, it is persistence and still short with a half-life of 4 to 49 days. Bentazon (technical) is only slightly soluble in water and is poorly volatile [3]but sodium bentazon, the form that is commercially available, is much more soluble. The accumulation causes the appearance of an important amount of highly reactive radical species, stories such as chlorophyll and oxygen alone, causing this stress. It is one of the most used herbicides in agriculture and gardening. It is resistant to hydrolysis and is not susceptible to abiotic degradation. The concern for human health is still very high so the monitoring of bentazon in the environment is constant, to avoid risks of contagion and to evaluate its potential carcinogenic effects. Residual amounts of bentazon have been monitored in water, soil, honey, plants, fruits and vegetables [4]. In addition, it has been reported as the disease affects health for animal living beings [5].

This pesticide can produce harmful effects in aquatic environments, being dangerous to the environment because it is highly mobile, with high potential for displacement in the soil and with great capacity to reach groundwater. The use of bentazon, a post-emergence herbicide, has become very popular for the control of weeds and broadleaf crops since 2003, following

the banning of atrazine in the EU. The application of this pesticide is carried out from both the ground and the air. Bentazon is classified, according to the World Health Organization (WHO) as a class III herbicide and its maximum concentration of bentazon admitted by the (WHO) in drinking water is 30μg·L^{-1}[6]. The mixture of herbs with other herbicides, such as Clorimuron, 2,4-DB, Imazaquin and Flumiclorac, cause their toxicity much greater sea for birds and fish, reaching a category II. WHO toxicological studies have shown that this pesticide has chronic toxicity. Although its degradation is relatively fast, bentazon and its metabolites are contaminants. It is harmful if swallowed or absorbed through the skin and causes irritation to eyes. Therefore, the removal of bentazon from water is necessary and the development of effective and inexpensive techniques for their removal has generated increased research interests in recent years. Among various water purification and recycling technologies [7-9], adsorption is one of the most efficient methods for removal of pollutants from water [10,11].

Different materials such as activated carbon, silica, titanium dioxide, alumina, and various nanomaterials such as nanometal oxides and carbon nanotubes are applied as adsorbent for removal of contaminants from aqueous solutions [12,13]. Activated carbon is very efficient in removing a variety of pesticides from surface and groundwater due to its high superficial area, large porous, good adsorption capacity, high thermal stability, good mechanical strength, fast kinetic, and versatility for removal of a broad type of inorganic and organic pollutants dissolved in aqueous media [14,15].Sorption to solid phases is a key process for the environmental fate of potentially toxic and bio accumulative pollutants. Adsorption is a simple, easy and economical method for removing substances from aqueous media and soils.

In this work, we use two different types of activated carbon, CAT and CARBOPAL, as low-cost adsorbent for the removal of pesticide from aqueous solutions. In literature has not been reported the use of these kind of activated carbon as adsorbents of any kind of pollutants. So, are novel substances with potential applications such as decontamination of surface and groundwater. Therefore, the purpose of this work is to evaluate the adsorption potential of CAT and CARBOPAL activated carbon for bentazonpesticide.

2. Materials and methods

2.1 Adsorbate

Technical grade bentazon of 99.9% purity was supplied by Sigma-Aldrich. The molecular structure of this pesticide is shown in Figure 1, with its acid-base equilibrium. A prior keto-enoltautomeric equilibrium explains this acid-base balance, generating a readily ionizable

species. The pKa of this species is 3.30. Figure 2 shows absorption spectrum of this substance in aqueous solution. Figure 3 shows speciation diagram of this molecule.

2.2 Adsorbents

Two types of commercial activated carbon were used, each one with different physical and chemical properties. Activated carbon were Hydrogen Sulfide CAT-Ox 4mm pellet Activated Carbon (UMI 2000) and CARBOPALMB 4S (Donau). Adsorbents were ground to the required particle size, 500–355 μm. First, they were washed with boiling water, to remove impurities in the inner pores and it was dried in oven at 110 °C for 24 h.Adsorbents names will be CAT and CARBOPAL, respectively, now on.Both carbonaceous materials used in the experiments were characterized to detail their surface and morphological chemical properties.

2.2.1 Adsorbents characterization

Figure 4 is an example of activated carbon surface studied, with acid and basic groups.The surface charges depend on the pH of the solution and the surface characteristics of the carbon. A negative charge results from the dissociation of acidic surface oxygen complexes such as carboxyl groups, phenolics, lactones and anhydrides. These surface acid sites are Bröwsted type. The origin of the positive surface charge and hence the basicity of the activated carbon is more uncertain because in carbon without nitrogenous functionalities, such as pyrroles, pyridines and amides, it may be due to basic surface oxygen complexes such as quinones, chromenes or due to the existence of rich regions in free delocalized π electrons from the nucleophilic zones of the polyatomic condensed ring.The textural characterization of the adsorbents was carried out by N_2 adsorption–desorption isotherms in automated adsorption equipment (Micromeritics ASAP 2020) at 77 K. The method of Barrett, Joyner and Halenda (BJH) is a method for calculating pore size distributions from experimental isotherms using the Kelvin model of pore filling. This model assumes that the pores are of slot type. It applies only to the mesopore and small macropore size range [16].For the specific study of micropores, the t-plot method was used [17]. FTIR spectrum of the solid was recorded by a ThermoNicolet FTIR spectrophotometer at the range of 400–4000 $cm^{-1}$with KBr as support. The zero-charge point (pH_{PZC}) is the pH value necessary for the net surface charge of the material is equal to zero. In this case, the zero point was determined using the mass titration method, according to ASTM D3838-05 (Standard Test Method for pH of Activated Carbon), based on measuring the pH as a function of the mass concentration of the solid [18-20]. To this end, samples of the dried activated carbon ranging from 0.1 to 1.0 g were placed in a flask. Then, 40 mL of previously boiled distilled water were

added. The system was boiled, during 15 min approximately. After this time, the system was disassembled and immediately, collecting the filtrate and measuring the pH at 50 ± 5°C. Finally, pH values were plotted as a function of the mass percentage, and the point of zero charge was determined by extrapolation to zero mass percentage.

Also, Boehm titration was performed, which is widely used for determination of acidic and basic surface groups of activated carbon [21]. Two bases were used for this purpose: NaOH and $NaHCO_3$. It is assumed that $NaHCO_3$ neutralizes only carboxyl groups while NaOH neutralizes carboxylic acids, phenols, lactones and carbonyls. HCl was used for neutralizing basic groups. 0.1000 g of carbon was placed in a 100 mL Erlenmeyer. 100 mL of 0.0563 MHCl solution was added. The system was kept under constant stirring for 24 h. After this time, the mixture was filtered and 20 mL of each solution was taken. They were titrated with 0.0539 MNaOH using phenolphthalein as pH indicator. For acidic groups, two measurements were made following the same procedure, using 0.0539M NaOH, and 0.0500 M $NaHCO_3$, and methyl orange as pH indicator. A blank experiment was also performed in order to verify the pH value of charcoal dispersion in distilled water.

Scanning electron microscopy (SEM) allows the study of the morphology of a solid surface by the incidence of an electron beam on it. The Scan Electronic Microscope (SEM) analyzes was performed on a JEOL JSM 6400 microscope, equipped with a thermionic cathode electron gun with tungsten filament and 25 kV detector. Samples are supported on brass discs by graphite tape, ensuring that they have been adequately dewatered prior to analysis.

Thermogravimetric (TG) analysis allows to determinate some functional groups on the surface of both materials. It is one of the techniques that makes use of temperature as a factor to be modified, and is based on the measurement of the mass variation of a sample when the sample is subjected to a temperature program in a controlled atmosphere. When a material is heated or cooled, its structure and chemical composition undergoes changes: fusion, solidification, crystallization, oxidation, decomposition, transition, expansion, sintering, etc. These transformations can be measured, studied and analyzed by measuring the variation of different properties of matter as a function of temperature. The thermogravimetric analyzes were carried out under inert conditions (nitrogen flow of 50 $ml \cdot min^{-1}$) and with a heating rate of 10 ° C min^{-1} to 1000 ° C. These analyzes were performed on a Seiko Exstar 6000 TGA / DTA 6200 thermobalance.

2.3 Sorption kinetics

For kinetic studies, 0.0020 g of adsorbent was contacted with 50 mL of 50 $mg \cdot L^{-1}$ of bentazon solutionin a thermostat system at 200 rpm and 293 K. At predetermined time intervals, the

adsorbent was allowed settled and 4 mL of solution was removed by filtered through 22 μm nylon filters, and their absorbance was measured by using UV spectrophotometer model at 252 nm. The amount of bentazon adsorbed q_t ($mg \cdot g^{-1}$), at time t (min), was calculated by Equation 1:

$$q_t = \frac{(C_o - C_t)}{W} V \quad [1]$$

where C_0 and C_t ($mg \cdot L^{-1}$) are the initial concentrations of bentazon and the bentazon concentration at time t, respectively; V(L) is the volume of the solution and W (g)is the used mass of dry adsorbent. A blank test of each system was also performed to verify that no adsorption occurred at the surface of the glass material.

2.4 Adsorption experiment

Discontinuous adsorption studies (batch process) were carried out by adding a fixed amount of activated carbon (0.0020 gr) into 25 mL Erlenmeyer flasks containing 20 mL of different initial concentrations (5–40 $mg \cdot L^{-1}$) of bentazon solution in aqueous solutions of NaCl0.01 M for each experiment. Distilled water was used to prepare all solutions and no buffer solutions were used to avoid possible formation of precipitates or competition with the solute in the adsorption equilibrium. The adsorption experiments were carried out at temperature and agitation controlled in a thermostat system at 200 rpm for 24 h. The initial and equilibrium bentazon concentrations were determined by absorbance measurement using double beam UV-vis spectrophotometer at 252 nm. It was then computed using standard calibration curve. The maximum capacity adsorption, q_e ($mg \cdot g^{-1}$), was calculated by Equation 2:

$$q_e = \frac{(C_o - C_e)V}{W} \quad [2]$$

where C_o and C_e ($mg \cdot L^{-1}$) are the liquid-phase concentrations of pesticide at initial and at equilibrium, respectively, V (L) is the volume of the solution and W (g) is the mass of the used dry adsorbent. Each assay was performed in duplicate.

2.4.1 pH effect

The importance of pH is related to the strong adsorption of the hydronium and hydroxyl ions, which compete with the solutes in the adsorption. In turn, the pH directly influences the net surface charge of the different materials and the degree of dissociation of the adsorbates by

modifying and controlling the electrostatic interactions between the two. A solution whose pH is lower than pH_{PCC} (zero loading point) or pH_{PIE} (isoelectric point) the surface will have positive charge; while a higher pH, the surface will have negative charge. The effect of pH does not follow a trend that can only be determined by knowing the structure of the solute, ie increasing or decreasing this value may increase or decrease the adsorptive capacity of a material. There are studies where both effects have been analyzed. To evaluate this factor, equilibrium isotherm was performing at four pH values (3.3, 5, 7 and 8) with the same pesticide concentration (5-50 $mg \cdot L^{-1}$) and adsorbent dosage (0.0020 g).

2.4.2 Ionic strength effect

Ionic strength is the other key factor that controls electrostatic interactions. Thus, these attractive or repulsive interactions can be reduced by the presence of ions in solution. This is due to a screen effect produced by the salt added on the surface loads. Therefore, when the electrostatic interaction between the surface and the adsorbent is repulsive, an increase in the ionic strength will increase the adsorption. On the contrary, when the electrostatic interactions are attractive, an increase in the ionic strength will decrease the adsorption [22]. Equilibrium isotherms were performed by changing the ionic strength of aqueous solutions by increasing concentrations of NaCl as support electrolyte. Ionic strength was maintained at 0.01 M, 0.30 M and 1.00 M, with the same initial concentrations (5-50 $mg \cdot L^{-1}$) and fixed adsorbent dosage (0.0020 g).

2.4.3 Temperature effect

The temperature was modified to calculate thermodynamic parameters, such as enthalpy change ΔH, entropy change ΔS and free energy of adsorptionΔG. Experiments were carried out under the same conditions, using the same initial concentrations (5-50 $mg \cdot L^{-1}$) and fixed adsorbent dosage (0.0020 g) at three different water bath temperatures of 293 K, 325 K and 341 K.

2.4.4 Computational studies

As the basic quantum chemical approach, we selected the density functional theory (DFT). This is one of the most efficient tools of quantum chemistry that enables one to calculate structural and energetic properties of relatively large systems. In this work, DFT calculations were performed using the Vienna Ab-initio Simulation Package [23, 24] including the dispersion interaction via Grimme's –D2 correction [25]. In this code plane wave basis sets are used to solve the Kohn–Sham equations. The electron projector augmented wave (PAW) method was used and the generalized gradient approximation (GGA) with the

Perdew–Burke–Ernzerhof (PBE) functional was utilized [26-31]. The fixed convergence of the plane-wave expansion was found with cut-off energy of 400 eV. A set of 3×3×1 Monkhorst-Pack k-points was used to sample the Brillouin Zone [32]. The ground state was found by a Methfessel-Paxton smearing of 0.2eV [33]. We have modeled the activated carbon slab. The atomic structure is similar to that of graphite consisting of three graphene layers arranged in a regular hexagonal pattern. In graphitic crystalline regions, the layers are stacked parallel to one another in a regular fashion. The atoms within a plane are covalently bonded (C-C bond length of 1.42Å) with sp^2 hybridization, while the interaction between the sheets occurs through relatively weak van der Waals forces, giving rise to a space between two graphene layers in graphite of about 3.35 Å [34]. During relaxation, the bottom layer of the slab are kept fixed in bulk positions to represent the semi-infinite bulk beneath the surface while the others was fully relaxed together with the pesticide molecule. The adsorption energy (Eads) was calculated as the difference between the energy of the adsorbed molecule and the sum of the free surface and the isolated molecule energies. A negative adsorption energy value indicates an exothermic chemisorption process. When analyzing the possible structures of the molecule adsorption complexes, we have selected diverse initial arrangements of the adsorbate molecule on the surface to ensure that we identified the lowest energy adsorbate/substrate structure. Here we present and discuss the most stable geometries obtained.

3. Results and discussion

3.1 Adsorbents characterization

3.1.1 Textural characterization

Table1 summarizes the pore diameter and surface area data for both CAT and CARBOPAL adsorbents. Specific surface and pore size was measured by BET method of N_2 adsorption isotherm. Results are shown in Figure 5 and Figure 6.It can be seen that CAT and CARBOPAL adsorbents are very different. The surface area and volume monolayer of CARBOPAL was found to be much higher than CAT activated carbon. The total pore volume is calculated from the amount of N2 adsorbed at P / P0 = 0.95, while the micropore volume is calculated by the Dubinin-Radushkevich method. The mesopore volume is also obtained from the N_2 adsorption isotherm in the range of relative pressures P/P_0: from 0.40 to 0.95 assuming the molar volume of liquid nitrogen is 35 $cm^3 \cdot mol^{-1}$. In the case of the medium pore size, they can be obtained from the Barrette-Joynere-Hanlenda method (BJH).

The value of C_{BET} is related to the degree of microporosity of the materials, where an increase in this value implies an increase in the degree of microporosity of the solids. There is no linear proportionality between the C_{BET} and S_{BET} values as can be seen in Table 1. In the case of CAT, whose value is much higher than CARBOPAL, it implies a high degree of microporosity in relation to the other materials. This can also be verified by the slope of its adsorption isotherm N_2. Also, the value of C_{BET} is related to the degree of interaction between adsorbate-adsorbent, where again an increase of this value implies that the interactions are stronger. That is, the more carbon microporous are those that have more interaction with the adsorbates and greater capacities of adsorption.

3.1.2 Boehm titration method

Table 2 summarizes the concentration obtained for acid and basic groups. CAT adsorbent present basic properties, while CARBOPAL has a surface with acidic characteristic.

3.1.3 Point of Zero Charge (pH_{PCC})

Table 2 shows these values. We could determinate that each adsorbent has different properties. CAT has Point of Zero Charge t equal to 7.46, which causes its properties to be fundamentally basic, while the CARBOPAL has a value of 4.76, being therefore more acidic. This difference of values is fundamental to analyze the interactions that are generated between each of the adsorbents and bentazon. This difference of values is fundamental to analyze the interactions generated between each of the adsorbents and bentazone, whose pKa value is 3.3. If the pH of the solution exceeds 4.76, both the bentazone molecule and the CARBOPAL surface will be negatively charged, whereas if the pH is higher than 7.46, the CAT will have a mostly negative charge.

3.1.4 FT-IR spectroscopy

Figure 7 shows the infrared spectra spectra of CAT and CARBOPAL commercial coals and Figure 8 shows FT-IR spectrum spectra for each material, respectively. Some differences can be seen in the curves, although both spectra are similar due to the carbonaceous nature of the adsorbents. In both cases a high intensity band is obtained at 3400-3500 cm-1, corresponding to hydroxyl groups and adsorbed water. In the case of CARBOPAL spectrum, this value is more intense, reason why it is possible to suppose that concentration of OH groups in this activated carbon is greater. Also, in the range of 1000 to 1260 cm-1 a pronounced peak is observed in both spectrums, indicative of C-O vibrations due to carboxilyc acid, alcohols and esters.

Unlike what is observed in the CAT spectrum, in CARBOPAL spectrum detects vibrations at 1600-1610 cm-1 and the band observed at 1461 cm-1 is attributed to the presence of carboxyl groups.(COOH). With the value mentioned in the previous range (1000-1260 cm-1),CARBOPAL has a greater number of functional groups of acid type, which explains the lower value of zero charge point, compared to the value of CAT (4,76 and 7,46, respectively).At 1453 cm-1, in the case of CARBOPAL, a small band due to the distortion of CH3 is observed. At 1600 cm-1there are not very pronounced bands due to C=C bond. At low values, between 800 and 950cm-1, are the vibrations of C-H in the aromatic ring appears in both spectrums. Peaks at aproximately 1582-1585 cm-1 were obtained in both materials indicating the C=O streching vibration of lactone and carbonyl groups

The bands found at 2850-2920 cm-1 in both spectra are characteristic of the presence of aliphatic groups. These peaks are not very intense, but are representative in this type of materials.

3.1.5 SEM microscopy

The morphological characterization of commercial coals has been performed. From Figure 9 we can confirm that a uniform structure is not observed for either of the carbonaceous materials.

3.1.6 Thermogravimetric analysis

This technique allows us to determine the functional groups, Figure 10 show the results. From Figure 10 a), the curve of the first derivative (shown in black) shows different depressions, which allow to explain the conformation of the starting material. In the temperature range between 80 and 100 ° C, the mass loss due to dehydration of the material, characteristic of all the solids studied by this technique, is detected. The loss of water is very significant. The temperatures at which CO and CO 2 species appear vary greatly depending on the type of carbon used, oxidation conditions and methods of analysis. Throughout the temperature range, reaching approximately 900 ° C, the mass losses are minimal, so that conclusions can be drawn on the composition of the material, where CAT does not present a great diversity of functional groups. Between 900 and 1000 ° C, a slight loss of mass is detected, due to the decomposition of quinones and carboxylic acids.

From Figure 10 b), as in the case of the CAT curve, CARBOPAL analysis shows a pronounced mass loss due to water molecules in the range of 80 to 100 ° C. It can also be postulated that surface oxygen structures are stable at temperatures below 200 ° C. Unlike the first TG and DTG, there is also a deep depression in the range between 600 and 850 ° C. The loss of mass at this temperature, giving rise to CO2, is then due to the decomposition of carboxyl, anhydrous and lactone groups. This is in agreement with the studies of the zero load point, where CARBOPAL presents a more acidic character than CAT.

3.2 Sorption kinetics

Kinetics of bentazon adsorption on both adsorbents was investigated by two models: the Lagergren pseudo-first-order model and the pseudo-second-order model [35-40].Figure11 shows the adsorption kinetics ofbentazon onto CAT and CARBOPAL. We can see that the values obtained for the experimental adsorption capacity (q_e^{exp}) are 526.3157 $mg \cdot g^{-1}$ and 325.161 $mg \cdot g^{-1}$ for CAT and CARBOPAL, respectively.

Lagergren proposed a method for adsorption analysis which isknown as the pseudo-first-order kinetic (Equation 3):

$$\log(q_e - q_t) = \log q_e - \frac{k_1}{2.303} t \quad [3]$$

where q_e($mg \cdot g^{-1}$)and q_t($mg \cdot g^{-1}$)are the bentazon adsorbed at equilibrium and t time respectively, and k_1 (min^{-1})is the adsorption rate constant of the pseudo-first-order. The linear plot of log (q_e-q_t) versus t gives k_1 as the slope and log q_e as the intercept, as shown in Figure14.

The pseudo-second-order kinetic model can be represented by Equation 4:

$$\frac{t}{q_t} = \frac{1}{k_2 q_e^2} + \frac{t}{q_e} \quad [4]$$

where k_2 ($g \cdot (mg \cdot min)^{-1}$) is the second-order adsorption rate constant. The linear plot of t/q_t versus t gives ($1 \cdot q_e^{-1}$) as the slope and ($1 \cdot (k_2 q_e^2)^{-1}$) as the intercept. Figure12 shows the linear plot on both adsorbents.

Results show that carbon CAT has the highest adsorption capacity at the equilibrium time of 120 minutes, while for carbon CARBOPAL presents much lower adsorption capacity at the equilibrium time of 50 minutes under the same system and this is correlated with k_2 values conditions (see Figures 12-14 and Table 3). Using both adsorbents, the model that best represents the kinetic process is the pseudo–second-order model. Due to the mesoporous characteristics of these two carbonaceous materials, the times of equilibrium reached are very credited, which makes them very good adsorbents.

$$\Delta q(\%) = \sqrt{\frac{\left[\left(\frac{q_{\exp} - q_{cal}}{q_{\exp}}\right)^2\right]}{N}} - 1 \quad \textbf{[5]}$$

3.2.1 Validity of kinetic model

Two different kinetics models were employed to understand the adsorption process. To compare fitting of the model, kinetic model was verified by the normalized standard deviation Δq(%) [41], which is defined as Equation 5:

where q_{cal}(mg·g^{-1}) and q_{exp} (mg·g^{-1}) are the calculated and experimental adsorption capacity respectively, and *N* is the number of points. The lower the value of Δq the better the model fits. Table 4 summarizes these values.

It can be see that the pseudo-second-order kinetic model yielded the lower Δq values. This is in agreement withobtained R^2 values and it proves that the adsorption of bentazon onto CAT and CARBOPAL could be best described by the pseudo-second-order kinetic model, which is based on the equilibrium chemical adsorption.

3.3 pH effect

The effect of pH on bentazon adsorption was studied under identical conditions using 25 mg·L^{-1} of initial concentration and pH 3–11 at 293 K for both adsorbent. Bentazon adsorption significantly changes over the studied pH range. The maximum adsorption capacity (q_e) decreases with increasing pH as shown in Figure15. The q_e decreases from 198.146 to 45mg·g^{-1} for an increase in pH from 3.5 to 10 on CAT, and from 73.205 to 4.545 mg·g^{-1} on

CARBOPAL. The same trend was obtained analyzing the adsorption isotherm at pH 3.5, 5, 7 and 8 from aqueous solution.

The behavior clearly suggests that adsorption of bentazon on both coals was dominated by the interaction between pesticide and adsorbent surface. This is opposed to the idea that materials with higher specific surface are those that have greater adsorptivity. At 5-10pH range, both CARBOPAL adsorbent (acidic surface with pH_{PZC}= 4.78) and bentazon (pK_a= 3.30) are negatively charged. Therefore, adsorption capacity is lower due to repulsive electrostatic interactions, as it is expected. On CAT, at pH range of 6-8 and 10-11, adsorptivity maintain almost constant, but decrease athigher pH values.It was found that the optimum pH is 3.3 for both adsorbent (natural pH).Results are like other studies, where the optimum pH for bentazon adsorption on other class of activated charcoal was the same [42] and similar results were obtained for other classes of substances usingdifferent adsorbents, where the increase in pH decreases adsorption [43-48].

3.4 Ionic strength effect

The effect of ionic strength on bentazon adsorption was studied at pH 5.3 on CAT where adsorbent and bentazon were oppositely charged (pH_{PZC} = 7.46 and pKa = 3.3) and pH = 2.6 on CARBOPAL where pesticide and activated carbon were equally charged (pH_{PZC} = 4.76). This situation can be confirmed with speciation diagram at Figure 3, where more than 99 % of bentazon is presented in anionic form. Theoretically, when the electrostatic forces between the adsorbent surface and adsorbate ions were attractive, as in this system, an increase in ionic strength will decrease the adsorption capacity. When the electrostatic attraction is repulsive, an increase in ionic strength will increase adsorption. We performed the isotherms with three different NaCl solution concentrations: 0.01 M, 0.30 M and 1.00 M. All experiments were made under the same temperature (293 K) and adsorbent dosage (2.0mg) of CAT and CARBOPAL, respectively. The effect of ionic strength is shown in Figures 16.

For both adsorbents, the increase of ionic strength causes a decrease in the maximum adsorption capacity. The increase on NaCl concentration produces an increase in the repulsive interactions between adsorbate and adsorbent due to the deprotonation of bentazon and the increased negative charge density on activated carbon surface.

3.5 Temperature effect

The temperature is a key factor affecting the adsorption process. Adsorption capacity decreases when increase the temperature. Carbon CAT reaches the maximum adsorption capacity at 391.65 $mg \cdot g^{-1}$(293 K) and 196 $mg \cdot g^{-1}$(341 K).On CARBOPAL, adsorption capacity decreases from 185.07 $mg \cdot g^{-1}$ at 293 K to 73 $mg \cdot g^{-1}$ at 341 K. These results are shown in Figure 17respectively. We have concluded that bentazon adsorption on both coals conduce an exothermic process. Similar results are found by Sadasivam et al and Netpradit et al considering different adsorbate-adsorbent systems [49-53].

On the other hand, the free energy (ΔG°) can be related with the equilibrium constant K_D (L mol^{-1}). The values of enthalpy (ΔH°) and entropy (ΔS°) for the adsorption process were calculated, using the following Equations 6-8:

$$\Delta G^{o} = \Delta H^{o} - T\Delta S^{o} \quad [6]$$

$$\Delta G^{o} = -RT \ln K_{eq} \quad [7]$$

$$\ln K_{eq} = -\frac{\Delta H^{o}}{RT} + \frac{\Delta S^{o}}{R} \quad [8]$$

In our experiment, the following method achieved adsorption equilibrium constants: as the bentazon concentration decreases, K_{eq} values are obtained by plotting a straight line of $\ln(q_e \cdot C_e^{-1})$ vs q_e based on a minimum square analysis and with extrapolation of q_e to 0. The intersection of the horizontal axis gives the value of K_{eq}. A Van't Hoff plot of $\ln K_e$ as a function of $(1 \cdot T^{-1})$ yields to a straight line. ΔH° and ΔS° parameters were calculated from the slope and intercept of the plot, respectively. It is assumed that adsorption occurs in multilayers on CARBOPAL. From which the value of maximum adsorption capacity (q_e) is obtained from the first plateau. Results can be seen in Table 5.The negative ΔG° values indicate that process is thermodynamically spontaneous. The negative value of ΔH° indicates that the nature of adsorption process is exothermic. This is also supported by the decrease in value of adsorbed capacity of the sorbent with the increase in temperature. The positive value of ΔS° shows the increased randomness at the solid/solution interface during the adsorption process.

3.6 Equilibrium modeling

Experimental data was tested to describe the experimental results with Langmuir, Freundlich and Guggenheim–Anderson–de Boer isotherm [54].

The Langmuir isotherm sorption monolayer assumes a surface containing finite active sites. Once one of these sites is occupied by a molecule is not possible that it interacts with other molecules. Langmuir isotherm has a hyperbolic dependence given by Equation 9:

$$q_e = \frac{Q_m K_{eq} C_e}{1 + K_{eq} C_e} \text{ [9]}$$

where Q_m is the maximum adsorption layer per unit mass of sorbent, K_L is the equilibrium constant for sorption reaction. Langmuir model is derived from a number of assumptions:

- All active sites have equal affinity for the sorbate
- Sorption is limited to a monolayer
- The number of sorbed species cannot exceed the number of active sites, it corresponds to the stoichiometry 1:1

Plazinski [55] shows that the Langmuir isotherm can be described from the equilibrium constant for the sorption sites with only occupation. The essential characteristics of the Langmuir isotherm can be expressed in terms of a dimensionless constant separation factor R_L that is given by Equation 10:

$$R_L = \frac{1}{1 + K_L Q_m} \text{ [10]}$$

where Q_m is the highest initial concentration of adsorbate (mgL^{-1}), and K_L (Lmg^{-1}) is the Langmuir constant. The value of R_L indicates the shape of the isotherm to be either unfavorable ($R_L>1$), linear ($R_L=1$), favorable ($0<R_L<1$), or irreversible ($R_L=0$). The R_L values between 0 and 1 indicate favorable adsorption.

Freundlich model assumes a heterogeneous adsorption, with active sites of the adsorbents which exhibit affinity sorbate distribution. Higher affinity sites are the first to be occupied. The model can be expressed by Equation 11:

$$q_e = K_F Ce^{\frac{1}{n_F}} \text{ [11]}$$

where $K_F$is the constant related to adsorption capacity and n_F is a parameter related to sorption intensity.

Guggenheim–Anderson–de Boer (GAB) model [56] (Equation 12) is frequently used in the fitting of experimental multilayer isotherms:

$$q_e = \frac{Q_m K_1 C_e}{(1 - K_2 C_e)[1 - (K_1 - K_2)C_e]} \quad [12]$$

where Q_m (mg·g^{-1}) is the maximum adsorption capacity on the first monolayer, K_1 and K_2(L·mg^{-1}) are the equilibrium constants for the first and the second monolayer, respectively. In order to simplify the calculation of the equilibrium, the formation of only two monolayers has been supposed. Results can be seen in Figure 18 and Figure 19 for each material.

In the case of CAT, GAB model was not analyzed because the formation of multilayers is not supposed. On CARBOPAL, model parameters and R^2 values presented in Table 6 indicate that GAB model showed the best correlation with experimental adsorption data. The shape of the curves on CARBOPAL indicates multilayer formation. The fraction of the CAT surface that is occupied by pesticide molecules (θ) can be calculated from the amount of pesticide adsorbed and the surface area occupied by one pesticide molecule (σ) using the Equation 13 [57]:

$$\theta = \frac{QmN\sigma 10^{-20}}{S_{BET}} \quad [13]$$

where θ represents the fraction of the surface that is occupied by pesticide molecules at saturation; Q_m (mol·g^{-1}) is the amount of bentazon adsorbed at saturation, as obtained from the Langmuir model; σ (Å^2·molecule^{-1}) is the surface area occupied by one molecule; N is the Avogadro's number (6.022 x 10^{23}); S_{BET} is the specific surface area of the adsorbent (946 m^2·g^{-1}). McClellan and Harnsberger have proposed an empirical relationship, Equation 14 that may be used for the estimation of σ for organic molecules adsorbed on activated carbon [57]:

$$\sigma = 1.091x10^{-16}\left(\frac{MW}{\delta N}\right)^{\left(\frac{2}{3}\right)} \quad [14]$$

where M_w is the molar mass of the adsorbed molecule (g·mol^{-1}); δis the adsorbate density (g·cm^{-3}) and N is Avogadro's number. Table 7 resumes the results.

3.7 Comparing with other carbonaceous materials

Adsorption capacity obtained for both materials was compared with other carbon adsorbents. Ayranci et al [58] analyzed adsorption equilibrium of bentazon on a different type of activated carbon, with a much larger specific surface area (named as Spectracarb2225, having a specific area of 2500m^2 g^{-1}). Adsorption capacity of this material achieved 100 mg·gr^{-1}, value much lower than those obtained for the materials used in our work. Salman, Njoku and Hameed also analyzed bentazonremotion onto banana stalk activated carbon [59]. In this work the authors achieved the lowest adsorption capacity: 80 mg·gr^{-1}. Omri et al [42] also studied bentazon adsorption on carbon prepared from Lawsoniainermis wood. In this work, the adsorption capacity achieved slightly exceeded the 120 mg·gr^{-1} at 293 K, also very lower to the values obtained with the CAT and CARBOPAL adsorbents. Omri et al also studied the effect of temperature, and the values are also much lower (between 100 and 70 mg·gr^{-1}). Salman et al also studied bentazon adsorption [60], and they achieved only 104,2 mg·g^{-1} at 303 K. This allows us to affirm that the materials studied in our work are superior as adsorbents for the removal of bentazon.

3.8 Computational results

It is known that dissociation of the bentazon molecule is affected by pH changes. Bentazon exists predominantly in anionic form under pH conditions near neutrality while the neutral molecule is the main specie in solution at low pH. The adsorption of both neutral and ionized forms of bentazon adsorbed on activated carbon model was studied by the VASP. DFT method is an efficient tool of quantum chemistry to calculate structural and energetic properties of large systems. The different on adsorption can be explained in terms of the pesticide structure and the surface behavior. At a given pH, the carbon surface and the adsorbate species may coexist in a complex system, resulting in some different adsorption schemes. In order to study the optimum adsorption geometry and the associated minimum energy, different initial adsorption geometries have been selected. Figure 20 shows the adsorption geometries for neutral bentazon, similar geometries were selected to study the adsorption of the ionized form of bentazon.

Given the aromatic structure, dispersion forces should be predictable between the π electron density of graphene layer on the activated carbon and the aromatic ring of the adsorbate. On the other hand, some specific localized interactions take also place from the polar groups of bentazon (i.e., carbonyl, sulfoxide -group). The decrease in the amount adsorbed at higher pH when anionic form predominant in solution is suggested by the weaker interactions of carbon surface with deprotonated bentazon than with its neutral form (the adsorption energies can be seen in Table 8). As pH is increased, the extent of dissociation of bentazon molecules is increased and the molecules become more negatively charged. The adsorption facility is reduced because carbon layer repels the bentazon anions reducing its contact to the carbon surface. It results in increased repulsion between molecule and surface leading to decrease in equilibrium adsorption (see Table 8). On the other hand, it is understandable to presume that bentazon is major stabilized and mainly trapped through π-π dispersive interactions with the aromatic ring moving toward to the carbon surface; it is confirmed by our DFT calculations that present the bentazon flat adsorption geometry as the most stable (see Table 8).

4. Conclusions

Adsorption equilibrium and kinetics of the bentazon pesticide on two different classes of activated carbon, CAT and CARBOPAL, was studied. Kinetics indicated that pesticide followed pseudo-second-order model on both adsorbent. Adsorption capacity decreases with the increase of temperature, pH and ionic strength variables. The adsorption capacity at 293 K was determined as 391.65 $mg \cdot g^{-1}$ and 185.07 $mg \cdot g^{-1}$ on CAT and CARBOPAL, respectively. Multilayers were formed on CARBOPAL, where the first layer has the strongest interactions. Experimental data adapt to Langmuir model on CAT and Guggenheim–Anderson–de Boer isotherm models on CARBOPAL. Adsorption of bentazon was found to be spontaneous at the temperatures under investigation (293-341 K) as indicated from the negative values of Gibbs free energy. Computational simulation shows that the possible interactions between the carbon surface and bentazon would be either dispersive interactions or electrostatic repulsion. As repulsion between molecule and surface is increased, the equilibrium adsorption energy leads to decrease. In general, bentazon is major stabilized and mainly trapped through π-π dispersive interactions when it is flat adsorbed on carbon surface. All these results show the efficiency of CAT and CARBOPAL

as potential materials for remediation of contaminated waters and ground waters with bentazon herbicide.

Acknowledgements

Financialsupportishighlyacknowledgedto Facultad de Ciencias Exactas-UNLP (Universidad Nacional de La Plata, Buenos Aires, Argentina), UTN (Universidad Tecnológica Nacional), UNS (Universidad Nacional del Sur), CONICET (Consejo Nacional de Investigaciones Científicas y Técnicas) and CIC BA (Comisión de Investigaciones Científicas de la Provincia de Buenos Aires). S. Simonetti, D. Ruiz and A. Juan are members of CONICET.

References

[1] Bruzzoniti M.C., De Carlo R.M., Rivoira L., Del Bubba, M., Pavani, M., RiattiM,Onida, B., EnvironSciencePollutantsResearchInt., 23, (2016), 5399-409.

[2] Office of Environmental Health Hazard Assessment California Environmental Protection Agency, Public Health Goal for Bentazon in drinking water, (1999).

[3] The pesticide manual, 9th ed. Worthing CR, (1991). Farnham, British Crop Protection Council.

[4] Feng X., Yu J., Pan L., Song G., Zhang H., Int J Environ Res Public Health.,13, (2016), 534.

[5]M. Abudayyak, S. Ozden, B. Alpertunga, and G. O¨ zhan", DrugChemToxicol, 37, (2014): 410–414.

[6] I.B. Müller, H. Willads Petersen, S.S Johansen, P Theilade, Forensic Sci. Int., 135 (2003), 235–236.

[7] M. I. Maldonado, S. Malato, L. A. Perez-Estrada, W. Gernjak, I. Oller, X. Doménech, J. Peral, J. Hazard Mater., 38 (2006) 363-369.

[8] S. Devipriya, S. Yesodharan,Energ.Mat. Sol. C, 86 (2005), 309.

[9] M. Sleiman, C. Ferronato, J. M. Chovelon, Environ. Sci. Technol.,42 (2008), 3018–3024.

[10] K. Y. Foo, B. H. Hameed, J. Hazard. Mater., 175 (2010), 1–11.

[11] Y. Lai, S. Chen,J. Chem. Eng. Dat., 58 (2013), 2290–2301.

[12] X. Ren, C. Chena, M. Nagatsu, X. Wang, Chem. Eng. J., 170 (2011), 395-410.

[13] F. Unob, B. Wongsiri, N. Phaeon, M. Puanngam, J. Shiowatana, J. Hazard. Mater., 142 (2007), 455-462.

[14] A. H. El-Sheikh, J. A. Sweileh, Y. S. Al-Degs, A. A. Insisi, N. Al-Rabady, Talanta, 74 (2008), 1675-1680.

[15] S. M. Taha, M. E. Amer, A. E. Elmarsafy, M. Y. Elkady, J. Environ. Chem. Eng., 2 (2014), 2013-2025.

[16]Galarneau A., Villemo, F., Rodriguez, J., Fajula, F., Coasne, B., Langmuir, 30 (44), 2014,13266–13274.

[17] Elliot P. Barrettl, Leslie G. Joyner, Paul P. Halenda, J. Am. ChemSoc, 73, (1951),3155–3158

[18] M.O. Corapcioglu, C.P. Huang, Carbon, 25, (1987) 569-578.

[19] J.S Noh, J.A Schwarz, Carbon, 5, (1989), 675.

[20] Y. Liu, Colloids Surfaces A, 320 (2008), 275-278.

[21] H. P. Boehm, Carbon, 32 (1994), 759–769

[22] I. Bautista-Toledo, M. A. Ferro-García , J. Rivera-Utrilla , C. Moreno-Castilla , and F. J. Vegas Fernández, Environ. Sci. Technol., 2005, 39 (16), 6246–6250.

[23] http://www.vasp.at/

[24] G. Kresse, J. Hafner, Phys. Rev. B 47 (1993) 558-561.

[25] S. Grimme, J. Comput. Chem. 27 (2006)1787-1799.

[26] G. Kresse, J. Hafner, Phys. Rev. B 48 (1993) 13115-13118.

[27] G. Kresse, J. Hafner, Phys. Rev. B 49 (1994) 14251-14269.

[28] J. P. Perdew, J.A. Chevary, S.H. Vosko, K.A. Jackson, M.R. Pederson, D.J. Singh, C. Fiolhais, Phys. Rev. B 46 (1992) 6671-6687.

[29] J.P. Perdew, J.A. Chevary, S.H. Vosko, K.A. Jackson, M.R. Pederson, D.J. Singh, C. Fiolhais, Phys. Rev. B 48 (1993) 4978-4978.

[30] P. Bloch, Phys. Rev. B 50 (1994) 17953-17979.

[31] G. Kresse, D. Joubert, Phys. Rev. B 59 (1999) 1758-1775.

[32] H. J. Monkhorst, J.D. Pack, Phys. Rev. B 13 (1976) 5188-5192.

[33] M. Methfessel, A.T. Paxton, Phys. Rev. B 40 (1989) 3616-3621.

[34] M. Sliwinska-Bartkowiak, H. Drozdowski, M. Kempinski, M. Jazdzewska, Y. Long, J. C. Palmer, K. E. Gubbins, Phys. Chem. Chem. Phys., 14 (2012) 7145-7153.

[35] Y. Liu, Colloids Surfaces A, 320 (2008), 275-278.

[36] H. Al-Johani, M. Abdel Salam, J. Colloid Interf. Sci., 360 (2011) 760–767.

[37] V. K. Gupta, I. Alib, Suhasa, V. K. Sainia, J. Colloid Interf. Sci., 299 (2006), 556–563.

[38] B. H. Hameed, I. A. W. Tan, A. L. Ahmad, Chem. Eng. J., 144 (2008), 235–244.

[39] M. Sarkar, P.K. Acharya, B. Bhattacharya, J. Colloid Interf. Sci., 266 (2003), 28-32.

[40] Y. Liu, L. Shen, Langmuir, 24 (2008), 11625–11630.

[41] X. Yang, B. Al-Duri, J. Colloid Interf. Sci., 287(2005), 25-34.

[42]A. Omri, A. Wali, M.Benzina,Arabian Journal of Chemistry, 9, (2016), 1729–1739.

[43] Y. Yang, Y. Chun, G. Sheng, M. Huang, Langmuir, 20 (2004), 6736-6741.

[44] S. Yahya Al-Degs , M. I. El-Barghouthi, A. H. El-Sheikh, G. M. Walker, Dyes and Pigments, 77 (2008), 16-23.

[45] Loux, M.M., Liebl, R.A., Slide, F.W.,,Weed Sci, 37 (1989), 712-718.

[46] A. Kumar Singh, S. Singh Cameotra, J Pet Environ Biotechnol., 4 (2013), 154-160.

[47] G. Shenga, Y. Yanga, M. Huangb, K. Yangb, Environ. Pollut., 134 (2005), 457–463.

[48] G. Newcombe G, Drikas M., Carbon, 35(1997), 1239-1250.

[49]S.Senthilkumaar, S.K. Krishna, P. Kalaamani, C. V. Subburamaan, N. GanapathiSubramaniam, Mod. Appl. Sci., 4 (2010), 67-83.

[50] S. Sadasivam, S. K. Krishna, K. Ponnusamy, G. SubramaniamNagarajan, T. W. Kang, S. Chandra Venkatesalu,J. Chem. Eng. Data, 55 (2010), 5658–5662.

[51] S. Netpradit, P. Thiravetyan, S. Towprayoon, J. Colloid. Interf. Sci., 270(2004), 255–261.

[52] V. K. Gupta, I. ALI, Environ.Sci. Technol., 42 (2008), 766–770.

[53] M. Dehghani, S. Nasseri, M. Karamimanesh, J. Environ. Health Sci. Eng., 2014 (2014), 12-28.

[54] K.Y. Foo, B.H. Hameed,Chem. Eng. J., 156 (2010), 2–10.

[55] W. Plazinski, Adv. Colloid Interf. Sci.,197-198 (2013), 58-67.

[56] E.A. Guggenheim, Application of statistical mechanics, Ed. Clarendon Press, Oxford, (1966).

[57] A. McClellan, H. Harnsberger, J. Colloid Interf. Sci., 23 (1967), 577-99.

58] Ayranci, E,Hoda, N., Chemosphere, 57, (2004) 755–762.

[59] Salman, J.M., Njokua, V.O., Hameed, B.H., Chemical Engineering Journal, 174,(2011) 41–48

[60] Salman, J.M.,Al-Saad, K., Int. J. Chem. Sci.: 10(2), (2012), 731-740.

Table 1. Physical properties of CAT and CARBOPAL.

Properties	CAT	CARBOPAL
BET surface area ($m^2 \cdot g^{-1}$)	983	1588
Average pore diameter (nm)	1	>0.8
Volume monolayer ($mmol \cdot g^{-1}$)	9.89	14.72

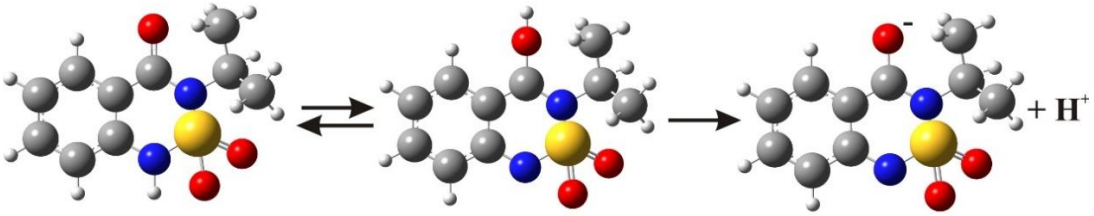

Fig. 1: Chemical structure of bentazon

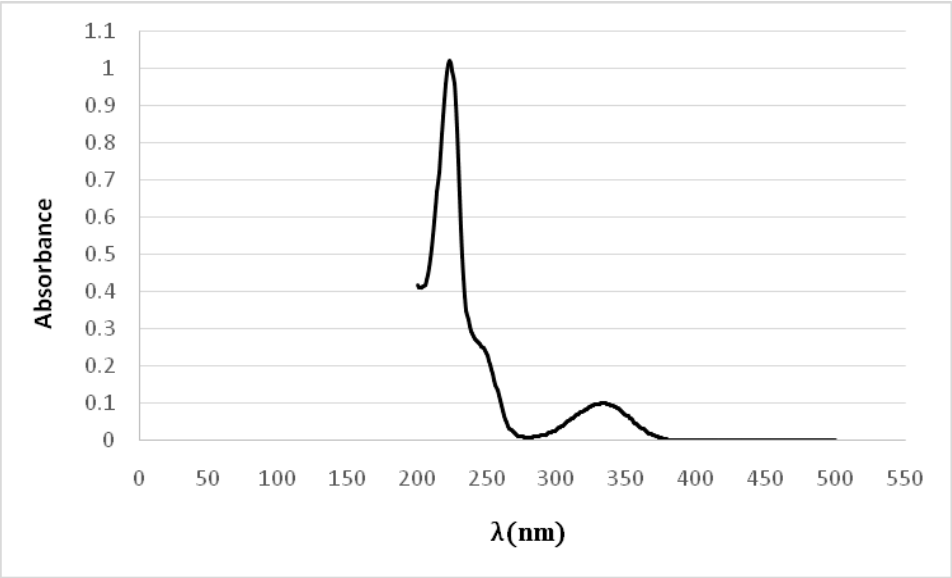

Fig.2: Absorbance spectrum of bentazon in aqueous solution

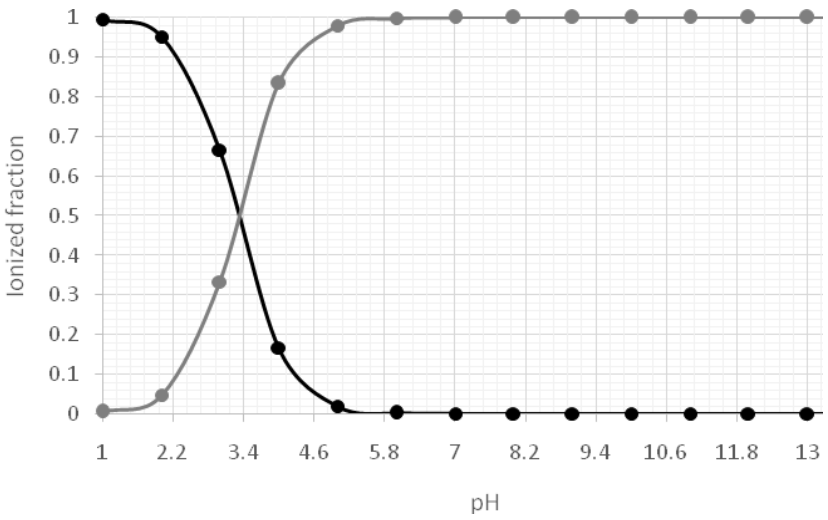

Fig. 3: speciation diagram of bentazon

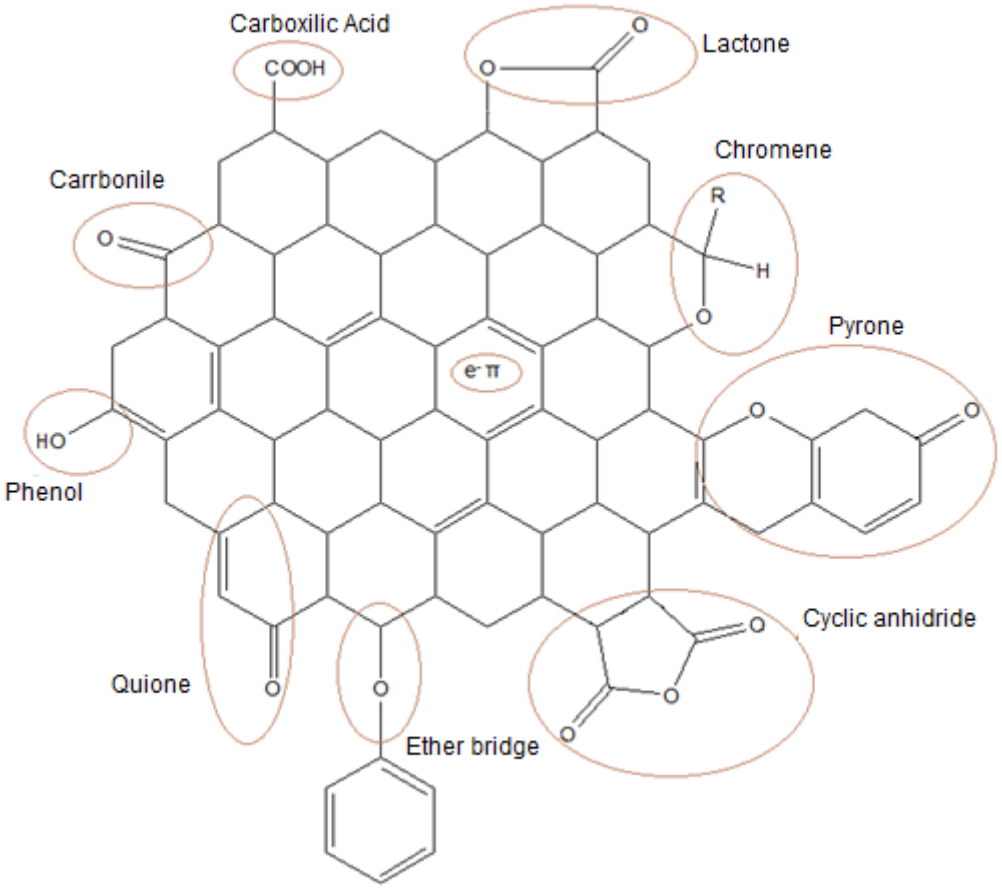

Fig.4: Representation of the surface of activated charcoal.

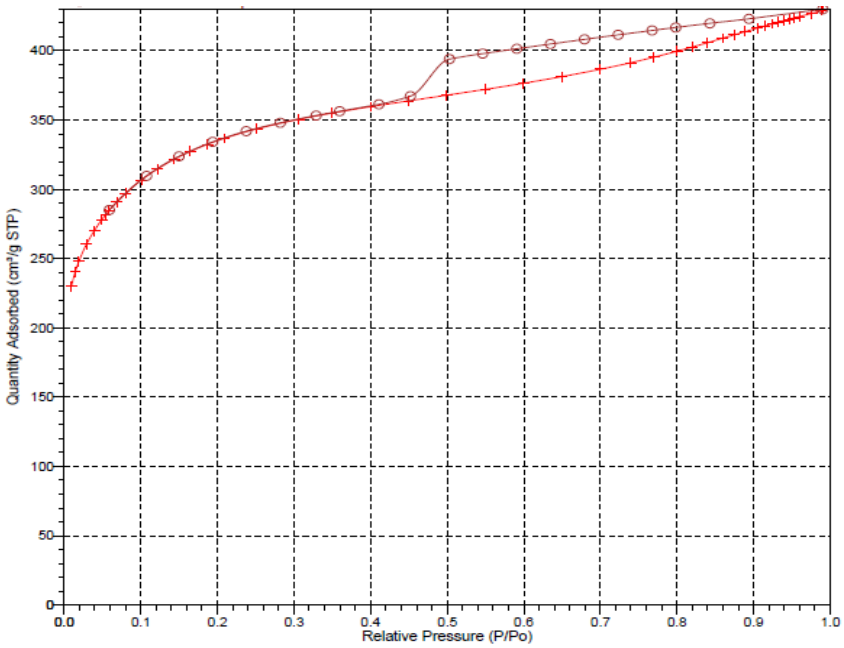

(a)

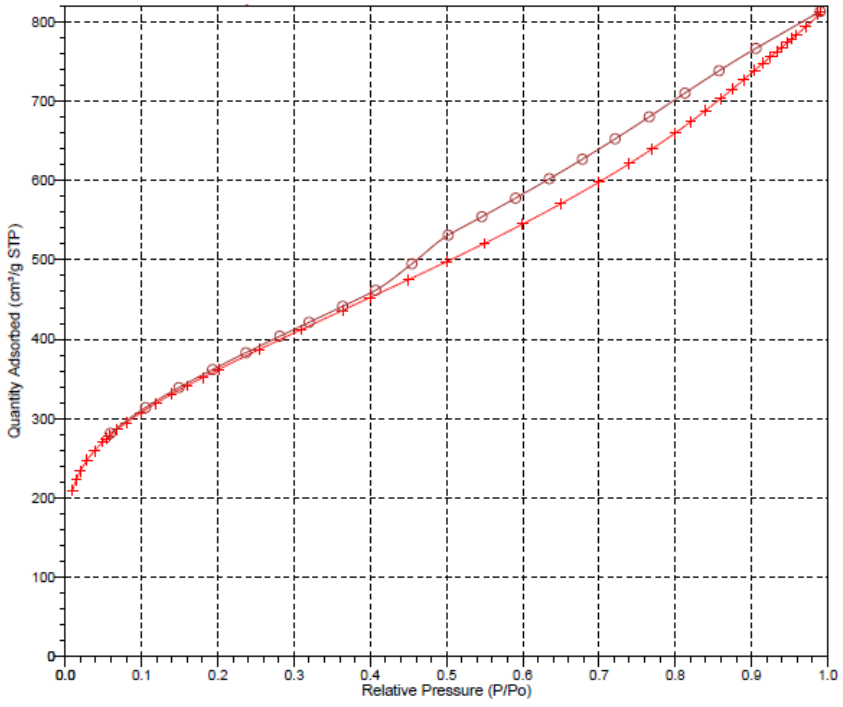

(b)

Fig. 5: N_2 adsorption-desorption isotherm of (a) CAT and CARBOPAL (b).

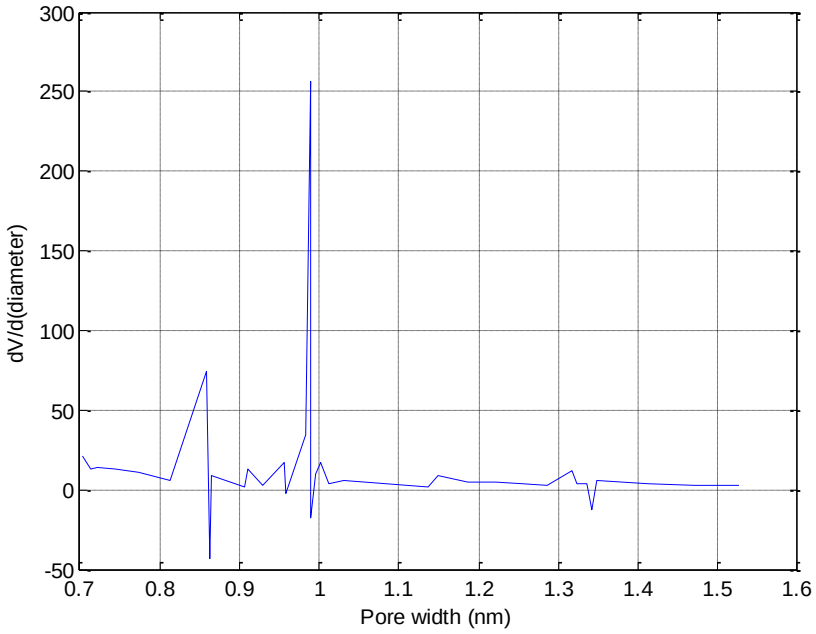

(a)

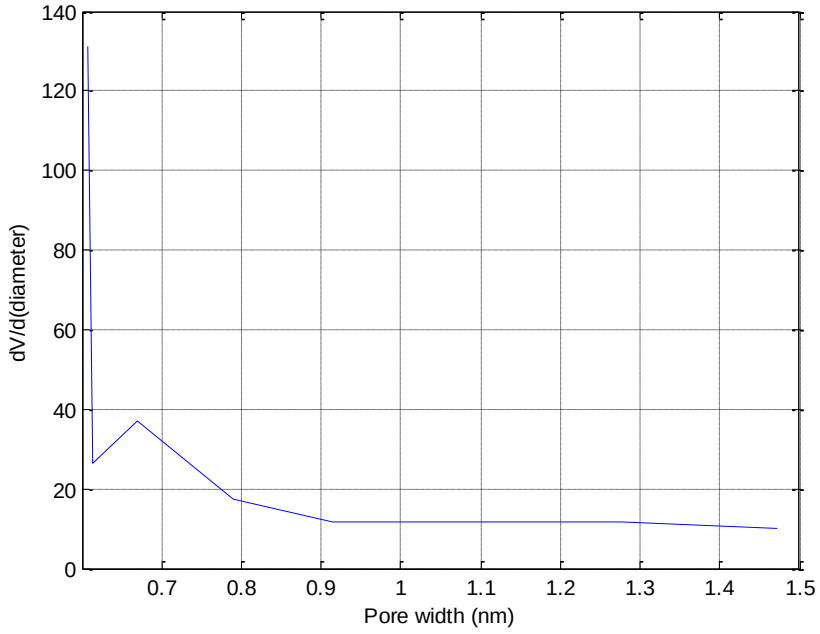

(b)

Fig. 6: Pore size distribution of (a) CAT and CARBOPAL (b).

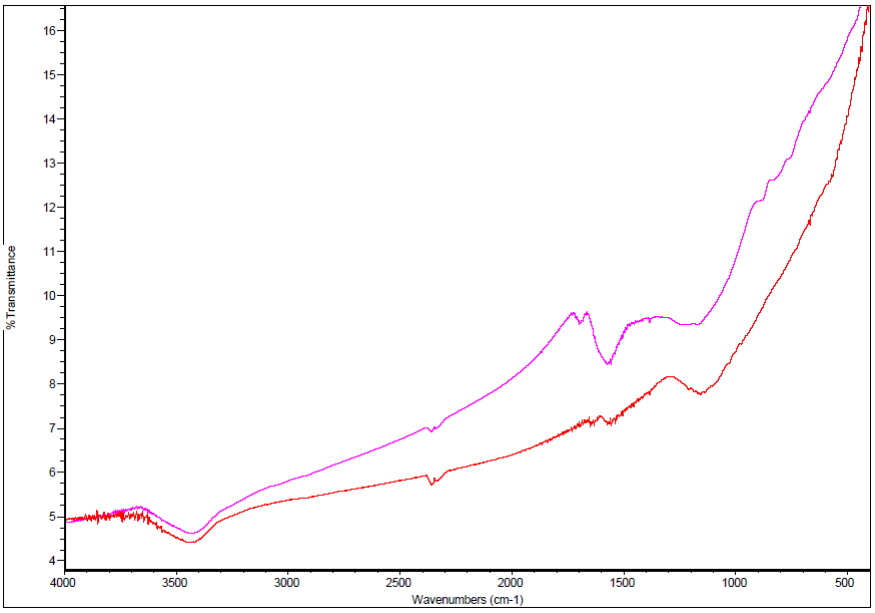

Fig 7: infrared spectra of CAT (pink line) and CARBOPAL (red line) commercial coals

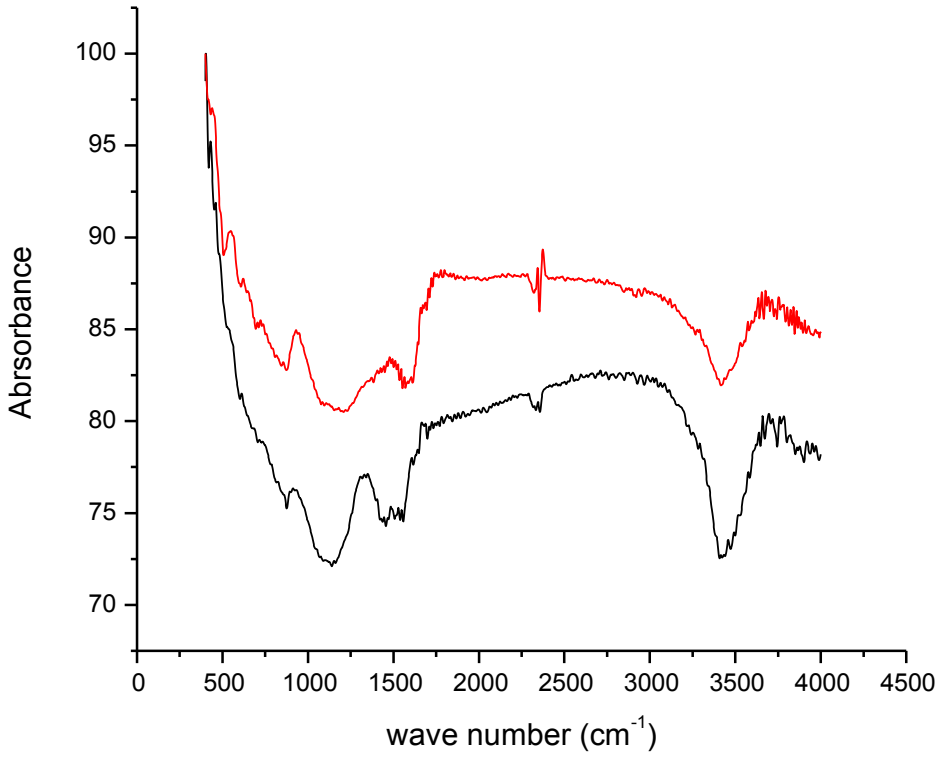

Fig.8: FT-IR of CAT (black line) and CARBOPAL (red line)

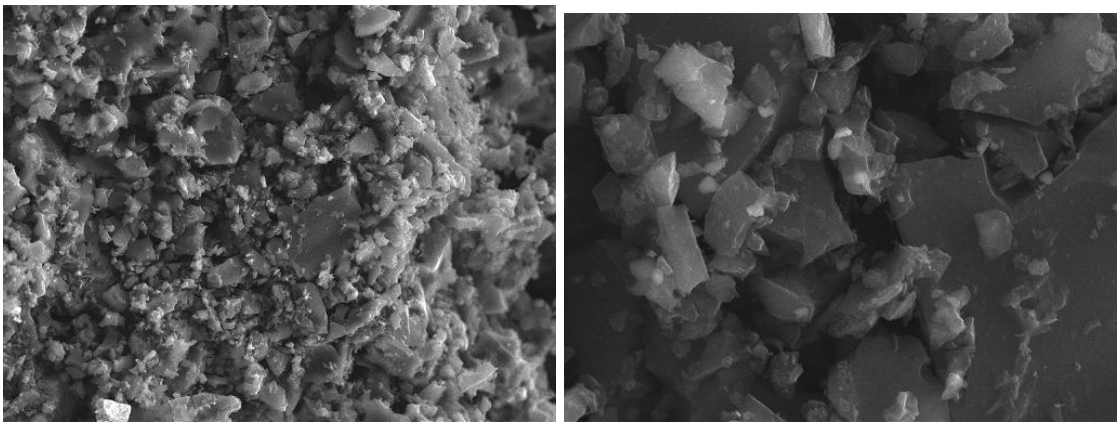

(a)

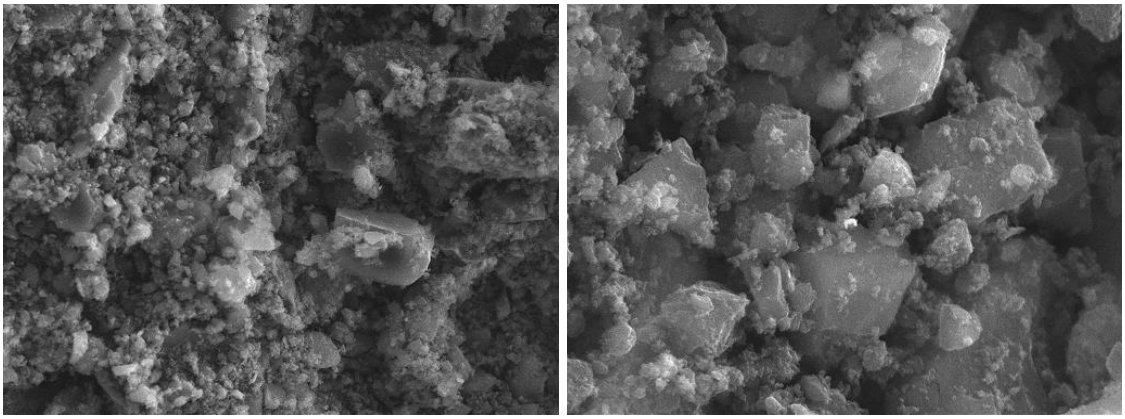

(b)

Fig.9: SEM images of CAT (a) and (b) CARBOPAL

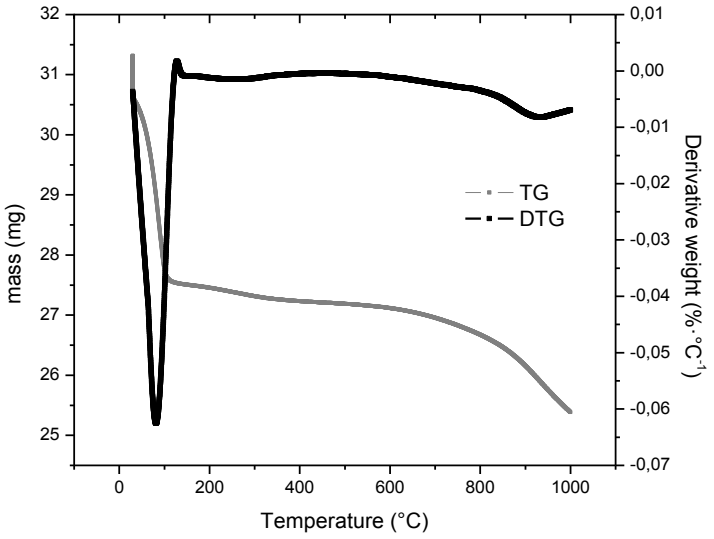

(a)

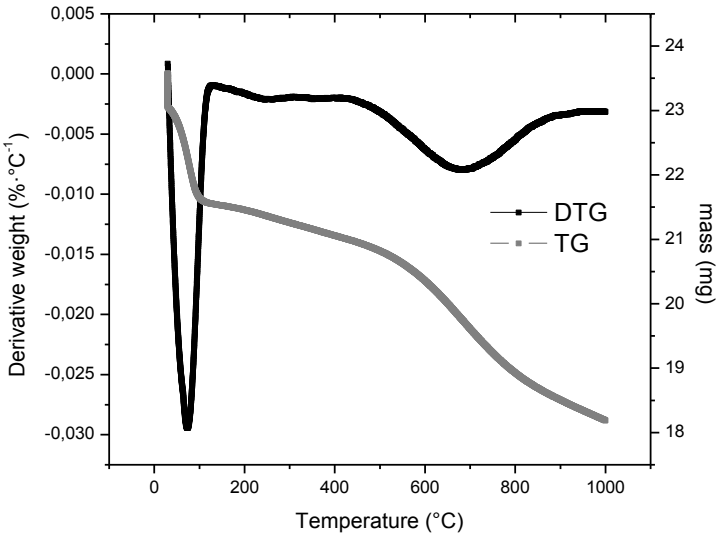

(b)

Fig. 10: TG and DTG spectrum of CAT (a) and CARBOPAL (b)

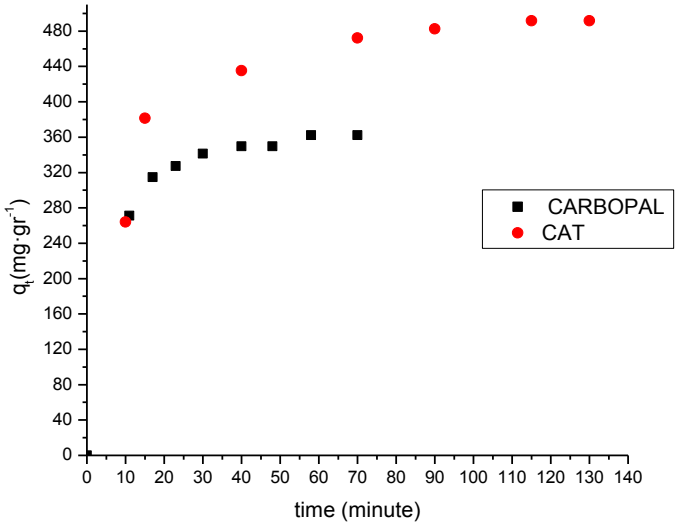

Fig.11: Adsorption kinetics of bentazon onto CAT and CARBOPAL

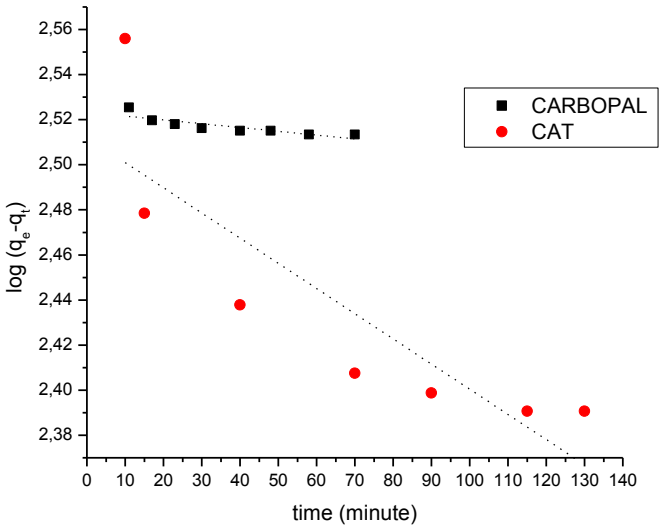

Fig.12: Pseudo-first-order kinetic for bentazonadsorption on CAT and CARBOPAL.

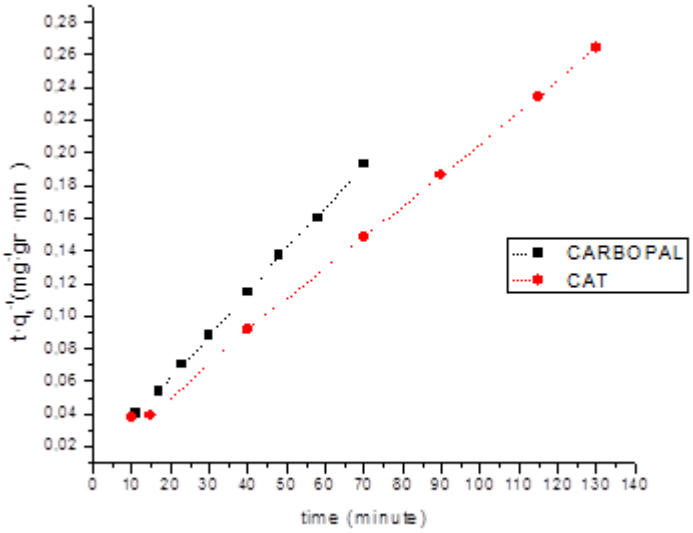

Fig.13: Pseudo-second-order kinetic for adsorption of bentazon on CAT and CARBOPAL.

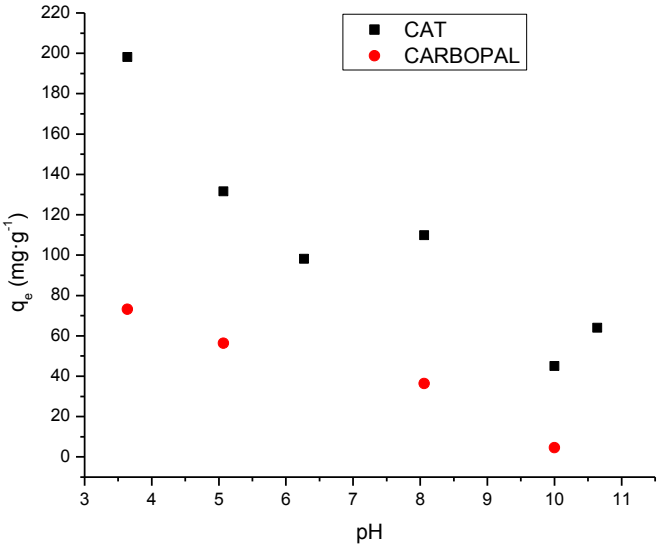

Fig.14. Effect of pH on equilibrium uptake of bentazon on CAT and CARBOPAL

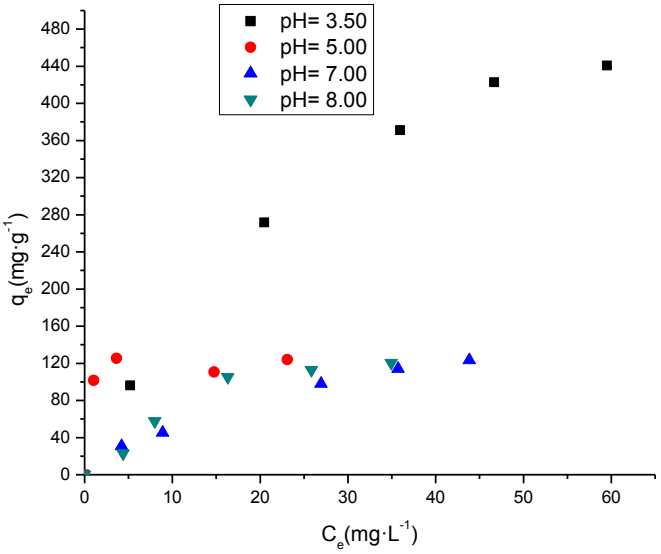

(a)

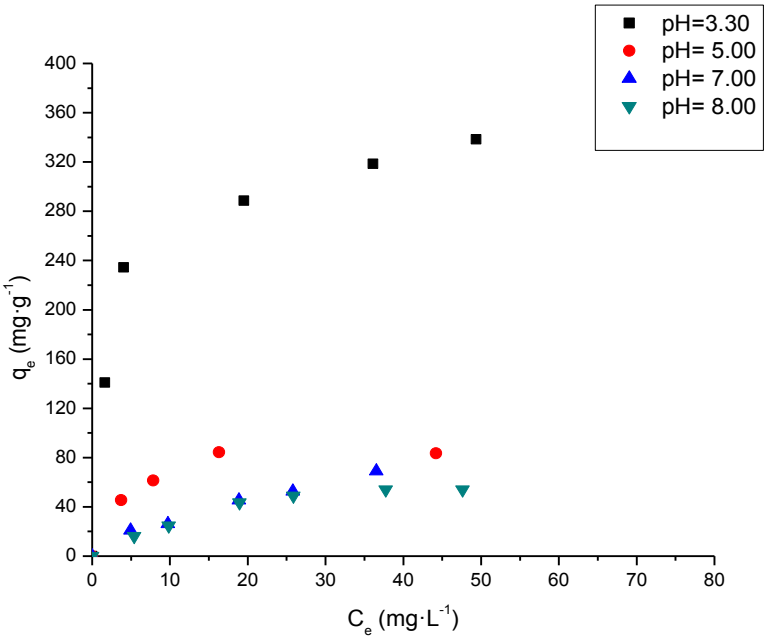

(b)

Fig.15: Isotherm on CAT (a) and CARBOPAL (b) at different pH

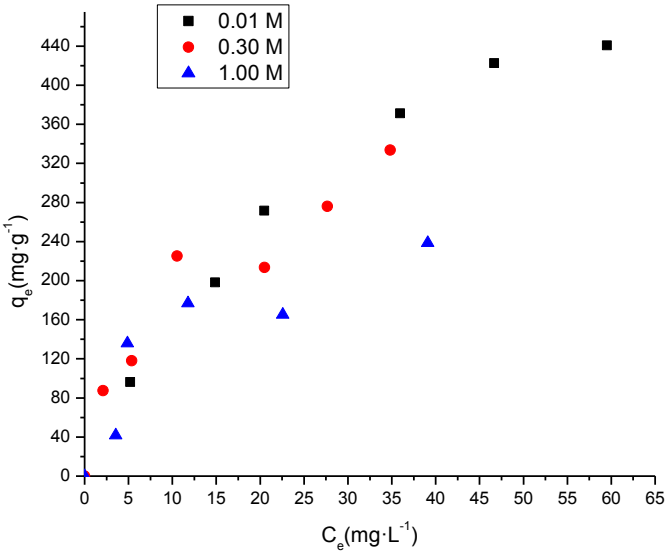

(a)

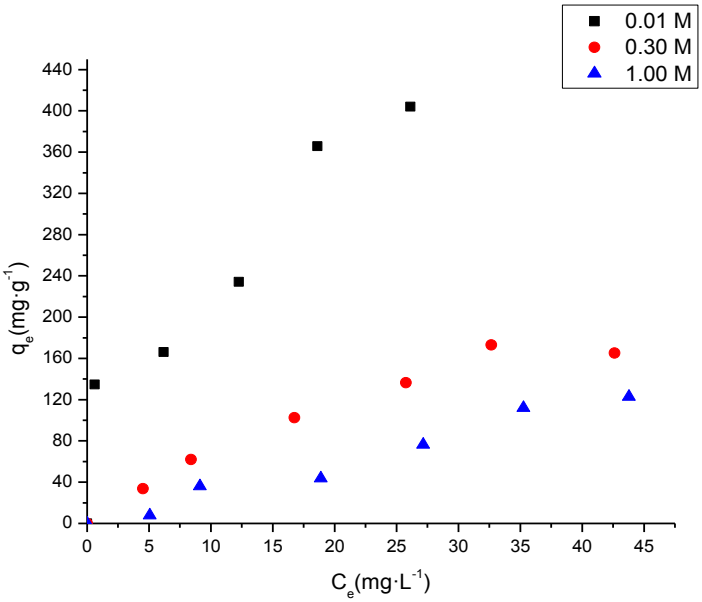

(b)

Fig.16: Adsorption isotherm on CAT (a) and CARBOPAL (b) with different ionic strength

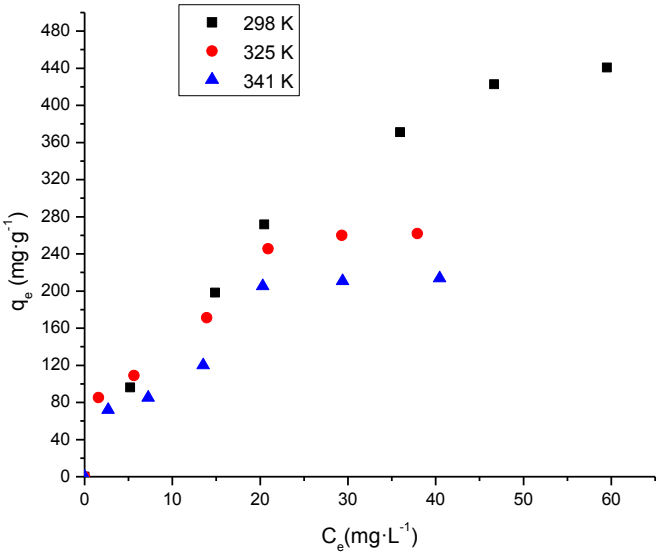

(a)

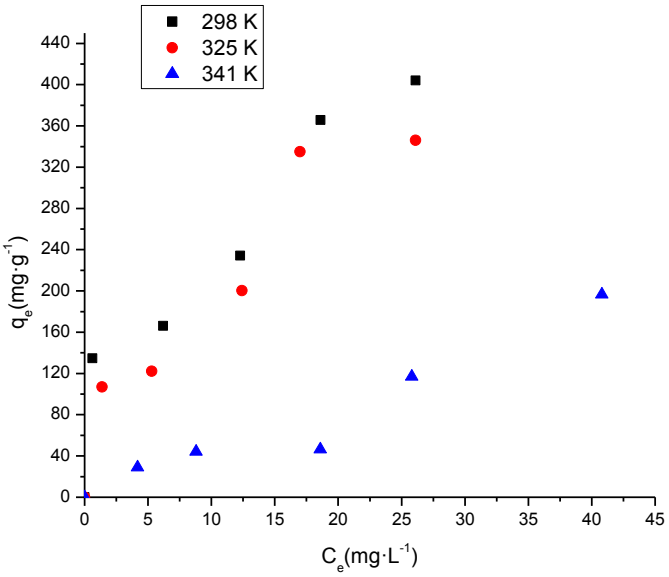

(b)

Fig.17: Adsorption isotherm on CAT (a) and CARBOPAL (b) at different temperatures: black dotes is at 298 K, red dotes at 325 K and blue dotes is at 341 K

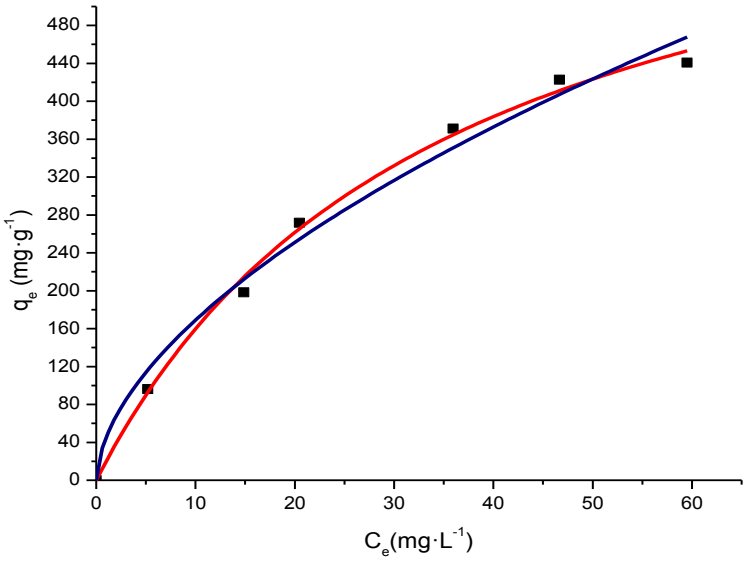

Fig.18: Adsorption isotherm modelling on CAT. Blue line represents Freundlich model and the red line represents the model of Langmuir

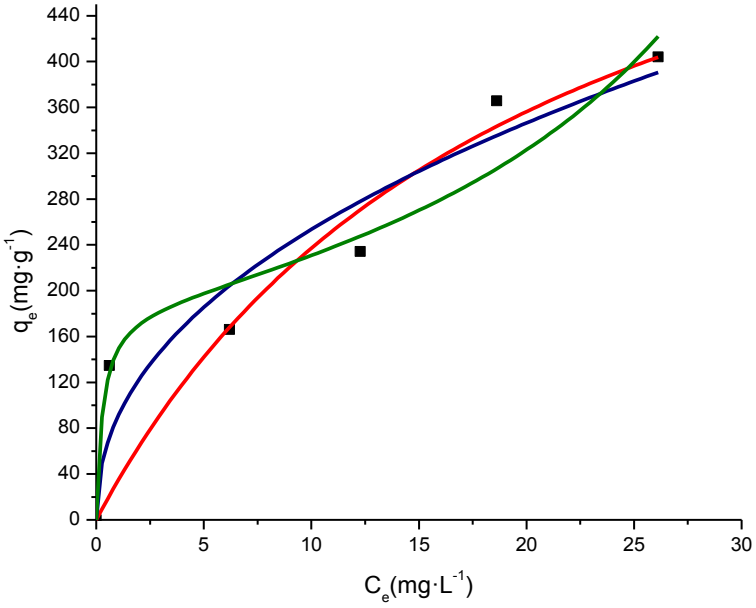

Fig.19: Adsorption isotherm modelling on CARBOPAL. Blue line represents Freundlich model, the red line represents the model of Langmuir and green is GAB model

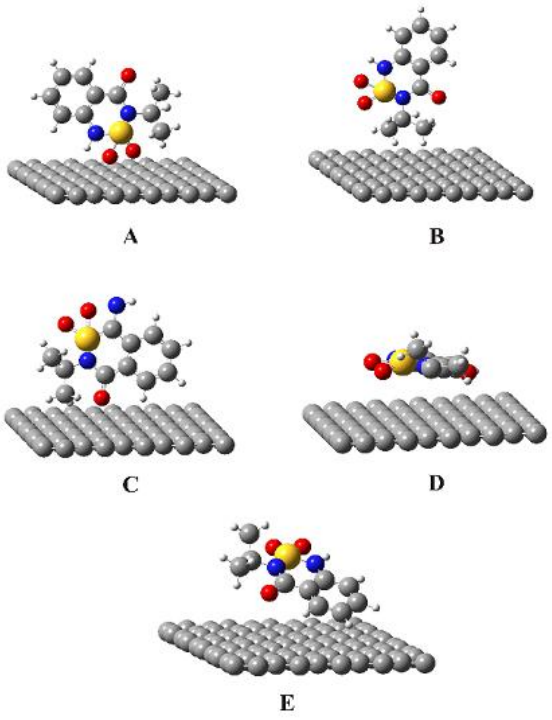

Fig. 20: Adsorption geometries for neutral Bentazon on activated carbon surface

Table 2. Adsorbents chemical properties.

Adsorbents	pH point of zero charge	[Carboxyl group]	[Phenolic group]	[Basic group]
CAT	7.46	2.721 mmol·g^{-1}	7.781 mmol·g^{-1}	2.441 mmol·g^{-1}
CARBOPAL	4.78	1.312 mmol·g^{-1}	7.922 mmol·g^{-1}	7.832 mmol·g^{-1}

Table 3. Kinetic model parameters for adsorption of bentazon onto CAT and CARBOPAL.

Kinetic model	CAT		CARBOPAL	
	Parameter	Value	Parameter	Value
Pseudo-first-order	$k_1(min^{-1})$ q_e^{cal} R^2	0.0368 126.037 0.9778	$k_1(min^{-1})$ q_e^{cal} R^2	0.0541 12.977 0.9329
Pseudo-second-order	k_2 $(g \cdot mg^{-1} \cdot min^{-1})$ $q_e(mg \cdot g^{-1})$ R^2	$4.862x10^{-4}$ 263.157 0.9993	$k_2(g \cdot mg^{-1} \cdot min^{-1})$ $q_e(mg \cdot g^{-1})$ R^2	0.0063 38.461 0.9996

Table 4. Normalized standard deviation for kinetics models.

Kinetic model	Adsorbent	
	CAT	CARBOPAL
Pseudo-first-order	Δq = 0.1989	Δq =0.3867
Pseudo-second-order	Δq =0.0287	Δq =0.3440

Table 5. Summarized thermodynamics parameters calculated.

Adsorbent	T (K)	ΔH (kJ·mol^{-1})	ΔS (kJ·K^{-1}·mol^{-1})	ΔG (kJ·mol^{-1})
CAT	293	-6.471	3.536x10^{-3}	-7.524
	325	-	-	-7.595
	341	-	-	-7.641
CARBOPAL	293	-15.672	1.045x10^{-2}	-18.734
	325	-	-	-19.069
	341	-	-	-19.236

Table 6. Resume values obtained for isotherm modelling for both activated carbons.

Isotherm model	CAT		CARBOPAL	
	Parameter	Value	Parameter	Value
Langmuir	Q_m(mg·g^{-1}) K_L(L·mg^{-1}) R_L R^2	720.544 0.0285 0.0464 0.9955	Q_m(mg·g^{-1}) K_L (L·mg^{-1}) R_L R^2	716.5946 0.0494 0.0152 0.8388
Freundlich	K_F (mg·g^{-1}) n_F R^2	45.4356 1.7525 0.9840	K_F (mg·g^{-1}) n_F R^2	89.858 2.22 0.9082
Guggenheim–Anderson–de Boer	Q_m(mg·g^{-1}) K_1 (L·mg^{-1}) K_2(L·mg^{-1}) R^2	- - - -	Q_m(mg·g^{-1}) K_1 (L·mg^{-1}) K_2 (L·mg^{-1}) R^2	185.07 3.515 0.0216 0.9230

Table 7. Values of σ and θ for adsorbed bentazon.

Material	σ (Å^2·molecule^{-1})	Q_m (mg·g^{-1})	S_{BET}(mg·g^{-1})	θ
CAT	43.715	391.655	946	0.436
CARBOPAL	43.715	185.07	1588	1.278

Table 8. Adsorption energies for neutral and ionized forms of bentazon on activated carbon.

Geometry (Fig. 20)	Neutral Bentazon (eV)	Ionized Bentazon (eV)
A	-0.45	-0.30
B	-0.64	-0.59
C	-0.90	-0.87
D	-1.39	-1.03
E	-1.23	-0.71